Influence of the specificities of ion irradiation on the nanostructural evolution in Fe alloys: an object kinetic Monte Carlo study

Monica Chiapetto[1,2], Lorenzo Malerba[1], Nicolas Castin[1], Cornelia Heintze[3], Charlotte S. Becquart[2]
[1]SCK•CEN, Nuclear Materials Science Institute, Boeretang 200, B-2400 Mol, Belgium
[2]Unité Matériaux Et Transformations (UMET), UMR 8207, Université de Lille 1, ENSCL, F-59600 Villeneuve d'Ascq Cedex, France
[3]Helmholtz-Zentrum Dresden-Rossendorf, Institute of Ion Beam Physics and Materials Research, Bautzner Landstraße 400, 01328 Dresden, Germany

Abstract

This work investigates the nanostructural evolution under ion irradiation in both a binary Fe-C alloy and an Fe-9%Cr-C alloy at 300°C, using an object kinetic Monte Carlo model originally developed to simulate neutron irradiation in Fe-(Cr)-C alloys. We studied the effect of specificities of ion irradiation that are expected to have an impact on the evolution of radiation-induced defect clusters as compared to neutron irradiation. The most relevant impact is due to the difference in dose-rate between neutron and ion irradiation. Moreover, the effect of two different ion irradiation regimes (continuous versus pulsed) on the nanostructure evolution material was also investigated: the presence of Cr was seen to lead to a different response over accumulated dose, the reason having been identified in the defect cluster recombination mechanism.

Introduction

High-Cr ferritic/martensitic (F/M) steels are candidate structural materials in the breeding blanket of future fusion reactors [1], as well as for fuel cladding and other core components in Gen-IV reactors [2, 3]. The Cr content in these steels is known to reduce radiation-induced swelling, typically by an order of magnitude [4-8] and is known to provide better resistance against corrosion [9]. However, F/M steels exhibit low-temperature (below 350-400 °C) irradiation hardening and embrittlement, which may make their use problematic under irradiation [10].

The limited availability of suitable neutron irradiation facilities, as well as the cost and time expenditure of neutron irradiation experiments, give rise to increasing interest in alternative irradiation sources, e.g. ion irradiation. Ion irradiation experiments have the great advantage of requiring only several hours of exposure to an ion beam to reach high irradiation doses, as opposed to several months or years of exposure typically associated with a neutron irradiation experiments. Another advantage of ion irradiation consists in the fact that relatively low energy ions, as opposed to neutrons, do not initiate nuclear reactions and do not produce unstable radioactive isotopes

during irradiation, hence not making the specimens radioactive. In addition, the experimental set up is much cheaper and parameters such as temperature can in principle be chosen freely and varied freely, and better controlled than in neutron irradiation experiments. Yet, drawbacks associated with ion irradiation experiments do exist. Important ones that concern specifically self-ion irradiation in Fe alloys are the small (of the order of a few microns) depth of penetration of ions into the material, the proximity of surfaces, the existence of strong damage gradients in defect concentrations throughout the specimen thickness, and the injection of an excess of interstitials with respect to vacancies. Moreover, the displacement rate is several orders of magnitude larger in ion than in neutron irradiation and this effect is likely to be exacerbated by the use scanning ion irradiation: in order to irradiate a larger specimen surface, the beam is focused on a small region and randomly moved to scan the whole surface, with the result that, locally, the material experiences an even higher dose-rate than the average one, followed by a time interval in which the irradiation is interrupted, as if the irradiation was pulsed.

The fact that the dose rate significantly influences the nanostructure produced in irradiated materials is well documented. Materials irradiated by neutrons at high dose rate show lower swelling than the same materials irradiated to the same integral dose at a lower dose rate [11-13]. Irradiation embrittlement resulting from exposure to high-energy neutrons shows sensitivity to the dose rate too, with lower irradiation dose rates giving rise to greater embrittlement [14]. Similarly, lower dose rate ion irradiation was also seen to stimulate phase decomposition of Fe–Cr alloys [15]. It is however a priori difficult to assess the effect of scanning versus using a defocused beam on the basis of these generic indications.

Computer simulation models offer in this context an effective way to explore the effect on microstructure evolutions of different ion and neutron irradiation conditions, providing some important hints for the interpretation of ion irradiation campaign results. In this work, using an object kinetic Monte Carlo (OKMC) model developed for neutron irradiated Fe-C [16] and Fe-Cr-C alloys [17], we first investigate the influence of the dose-rate on the formation and growth of radiation-induced defect clusters. As a second step, the effect of pulsed versus continuous ion irradiation at ~300 °C, is also addressed. In previous simulation work it was shown that the reduced mobility of SIA clusters with Cr is the most important parameter driving the microstructure evolution of F/M steels under neutron irradiation [17, 18]. Here we find that the presence of Cr may also be key to explain the different response under pulsed versus continuous ion irradiation in F/M alloys.

Method and parameterization

For all our simulations we started from the parameterizations for Fe-C and Fe-9%Cr-C fully reported, respectively, in [16] and [17]. We used the Object kinetic Monte Carlo (OKMC) model MATEO, recently developed at SCK●CEN (Mol, Belgium) and which showed to be equivalent to the OKMC code LAKIMOCA used in our previous works [16-18] and thoroughly described in [19]. The approach we adopted is explained in detail in [16, 17, 20], but for convenience we highlight here the fundamental ideas.

The OKMC is a stochastic method used to describe the evolution of defects and their clusters in materials subjected to irradiation, disregarding the detail of processes directly involving atoms and focusing instead only on the properties of defects, treated as objects. Neutron and ion irradiation produce point defects, namely vacancies (Va) and self-interstitial atoms (SIA), which may form clusters. The objects we consider are therefore Va and SIA clusters or any other nanostructural feature that needs to be included, like carbon (C) atoms or carbon-vacancy (C_2V, see [16]) complexes

which act as immobile spherical traps for mobile defects). All objects are located in a simulation volume in which their coordinates are known and tracked. Every object introduced in the system has an associated spherical reaction volume, with the exception of large dislocation loops (> 150 SIA) which are represented by toroids: when the reaction volumes of two objects overlap a predefined reaction, like clustering between same type defect clusters or annihilation between a Va and an SIA, takes place.

It is important to note that Cr atoms are not introduced explicitly in our model, but their presence is reflected in the change of the mobility of SIA objects, i.e. applying a "grey alloy" approach (see [17] for further details). This choice was dictated by the need to avoid the introduction of an unnecessarily large number of objects in the system that would have slowed down enormously our simulations, together with the lack of data about solute-defect interaction mechanisms.

SIA and Va single defects and clusters are thus the only objects that can migrate within our system and the probabilities that define the occurrence of an event (e.g. defect migration, recombination, clustering, de-trapping or emission of single defects from bigger clusters) are predefined in terms of Arrhenius frequencies for thermally activated processes:

$$\Gamma_i = \nu_i exp\left(\frac{-A_i}{k_B T}\right) \quad (1)$$

Here ν_i is the attempt frequency (alias the prefactor) of the event *i;* A_i is the corresponding activation energy, which must embody both the thermodynamics and the kinetics of the system being studied; k_B is the Boltzmann's constant and T is the irradiation temperature expressed in K. For every simulation step, among the N possible events, only one is chosen, based on the corresponding probabilities defined by the parameterization and according to the stochastic Monte Carlo algorithm [21]. Time elapses according to the residence time algorithm, where at each simulation step the time increase is obtained as inverse of the sum of all the frequencies Γ_i associated with each of the N possible independent events [22]:

$$\Delta t \propto \frac{1}{\sum_1^N \Gamma_i} \quad (2)$$

In the model we also have two kinds of pre-existing sinks for Va and SIA defects: grain boundaries and dislocations. Grain boundaries act as a spherical surface sink for defect clusters of all sizes and the absorption of defects is taken into account by applying the algorithm described in [23], here briefly described. Each object has two sets of coordinates, one, subjected to periodic boundary conditions, that expresses its position in the simulation box, and a second one, not subjected to periodicity, that expresses its distance from the centre of a supposedly spherical grain. Migrating objects are absorbed by grain boundaries as soon as one of the following situations occurs: i.) the object reaches the grain boundary, or ii.) the distance travelled by the object equals the grain radius, irrespective of its position inside the box. Thus, for sake of simplicity, in our OKMC model the concept of grain size is translated into a diameter.

Dislocations are reproduced in our model by immobile spherical sinks randomly distributed in the simulation volume: their number and size are chosen in such a way that the sink strength associated with them equals the one due to the corresponding material dislocation density [24].

When simulating the damage production from neutron or ion irradiation, debris of cascades containing Va and SIA objects of different sizes or residual Frenkel pairs (i.e. simple SIA–Va pairs) are randomly introduced in the system. The impinging flux is thus transformed into a production rate, directly corresponding to a well-defined dpa rate, of randomly distributed displacement cascades of different energies which are chosen from a database [25-27] of displacement cascades that were

simulated using molecular dynamics (MD). The accumulated dpa is eventually calculated using the NRT formula [28]. In the case of neutron irradiation, cascade energies ranging from 5 to 100 keV were considered [17, 29], while in order to simulate ion irradiation only cascade up to 20 keV were used, to take into account the lower energy spectrum of primary knock-on atoms produced by self-ions in Fe. Since the volume of the simulation is much smaller than the penetration range of the ions, the simulation is performed assuming that both the surface and the interstitial injection peak are sufficiently far away to be able to neglect their influence; moreover, the volume is considered to be small enough to neglect damage profile gradients.

The two materials were simulated by associating to them a C/C-Va complex content of, respectively, ~15 [17] (Fe-9%Cr-C) and ~100 appm (Fe-C) [16]. The corresponding grain diameters were of 20 and 250 µm, and the dislocation density 6.3×10^{13} [30] and 7×10^{13} m^{-2} [31].

The two irradiation profiles, continuous and pulsed, were considered, as schematically represented in Figure 1: a continuous ion flux of 1.33×10^{-11} $cm^{-2}s^{-1}$, corresponding to 5×10^{-5} dpa/s at a depth of 500 nm [32], and a pulsed ion beam characterized by three pulse packets of height 9.18×10^{13} $cm^{-2}s^{-1}$ (3.45×10^{-2} dpa/s) applied every ~19.2 ms. The mean dpa-rate calculated in the pulsed case equals the dpa-rate applied in the continuous irradiation case. Taking as a reference the technical features of the ion irradiation equipment available at HZDR (Germany), The length of each pulse was taken to be ~0.015 ms, with a time between pulses of ~0.5 ms [32]. In the lapses of time between successive pulses or packets the material was simulated to be subjected to annealing at the constant temperature of ~300 °C. The two irradiation profiles were chosen to be equivalent in terms of accumulated dose (0.1 dpa) after a 33-minute ion irradiation.

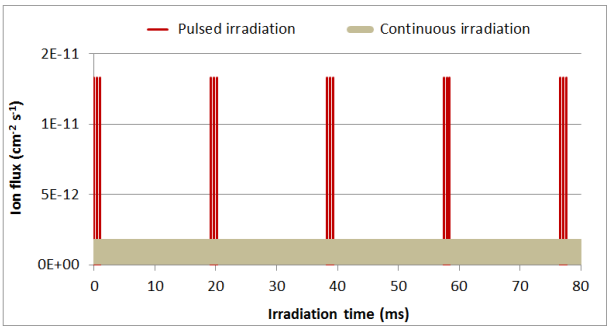

Figure 1: Schematic representation of the two investigated irradiation profiles.

All simulations were performed with periodic boundary conditions in the three directions, in a box of size 600×750×1000 a_0^3 (with a_0 =2.87×10^{-10} m the lattice parameter of α- Fe), chosen non-cubic in order to avoid potential anomalies from 1D-migrating SIA clusters (i.e. clusters > ~5 SIA) entering a migration trajectory loop [33].

Results

Dose rate effect under continuous irradiation

Figure 2 shows the SIA defect cluster number density (left) and mean size (right) evolutions over dose up to 0.06 dpa in the Fe-9%Cr-C model alloy, when two different fluxes are applied at an irradiation temperature of ~300°C: (1) a dose-rate of 10^{-7} dpa/s, corresponding to the typical neutron flux of a materials test reactor such as BR2 in Mol, Belgium, and (2) a dose-rate of 5×10^{-5} dpa/s,

corresponding to the continuous ion flux typical of self-ion irradiation in Fe [32]. The analysis of the simulation results was conducted dividing the SIA cluster population into two groups: SIA loops that are potentially visible in the transmission electron microscope (TEM) and SIA clusters corresponding to sizes below the TEM visibility threshold (~1.3 nm in diameter [34], equivalent to ~90 SIA per cluster). Our model predicts higher defect number densities at the higher irradiation dose-rate, the difference reaching about one order of magnitude at ~0.06 dpa for both SIA groups: this is a consequence of the reduced absorption at sinks of small SIA defect cluster, which also constitute possible nucleation points for the creation of bigger SIA clusters throughout the irradiation process, due to the shorter lapse of time between successive cascades at higher flux. A similar trend was already reported in [18], where an OKMC study over the effect of dose-rate in F/M steels was performed. From Figure 2 it is also possible to see that the formation of bigger SIA clusters is enhanced at the lower dose-rate (10^{-7} dpa/s): thus, a redistribution in size towards bigger SIA clusters occurs at the lower dose-rate as a consequence of the combined effect of higher likelihood for mobile SIA clusters to be trapped (by C and C_2V complexes present in the matrix) and higher probability to reach another SIA defect and grow up to visible TEM sizes, because of the longer time elapsing before a new cascade is introduced in the neighbourhood of a migrating SIA cluster.
The microstructure evolution of Va defect cluster population also showed similar trends as in the SIA case, with a higher defect number density at the higher dose-rate.

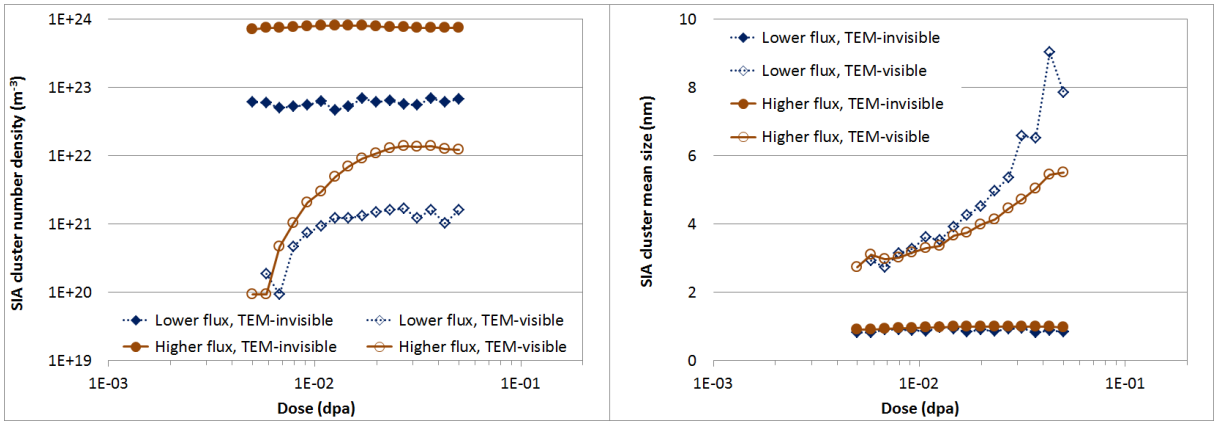

Figure 2: SIA defect cluster number density (left) and mean size (right) evolutions over dose in Fe-9%Cr-C at 300°C for two dose-rates: 10^{-7} dpa/s (lower flux) and $5{\cdot}10^{-5}$ dpa/s (higher flux). Loops are considered visible in TEM if their radius is larger than ~1.3 nm (90 SIA) [34].

The nanostructure evolution predicted by our model is in broad accordance with experimental TEM observations performed on the same F/M model alloy irradiated with both neutrons and ions at 300 °C [34]: in both cases the formation of dislocation loops was observed, but the total number density was about 5 times higher after ion irradiation. Differences were also observed in terms of cluster size: smaller loops were observed in the ion-irradiated materials, about 3 nm, compared to the 5 nm in the case of neutron irradiation [34].

Pulsed versus continuous ion irradiation

Figure 3 shows a comparison between the nanostructure evolution versus dose at ~300 °C in Fe-C (above) and Fe-9%Cr-C (below) when pulsed or continuous ion irradiation is applied. The SIA cluster population number density (left) and mean size (right) trends are reported.

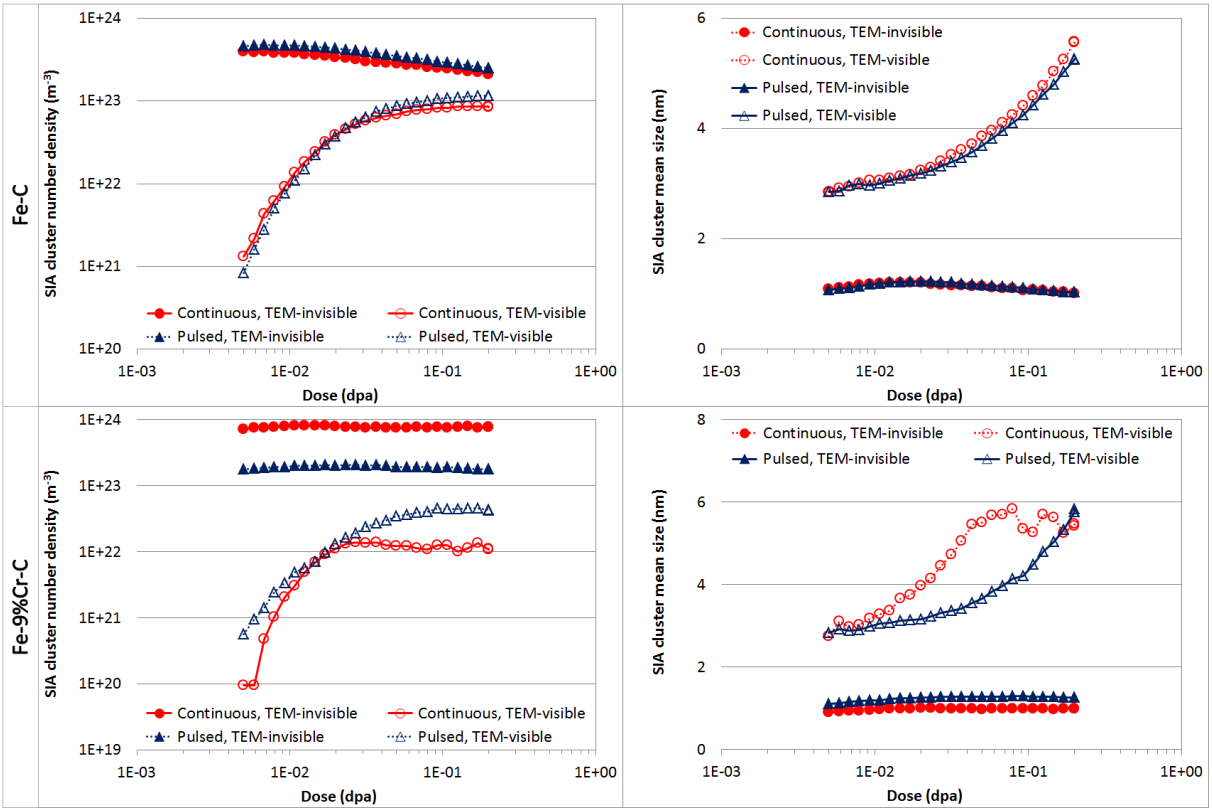

Figure 3: Comparison of the SIA cluster nanostructure evolution with accumulated dose at ~300 °C in Fe-C (above) and Fe-9%Cr-C (below) under pulsed and continuous ion irradiation (average dose rate $5 \cdot 10^{-5}$ dpa/s in both cases). SIA loops are considered visible in TEM if their radius is larger than ~1.3 nm (90 SIA) [34].

The most remarkable result is that in the Fe-9%Cr-C model alloy pulsed and continuous irradiations induce a different nanostructure response in terms of defect cluster number density and mean size evolution with accumulated dose, which is not observed in the Fe-C alloy. More specifically, under continuous irradiation higher number densities for small SIA defect clusters as well as the formation of bigger TEM-visible clusters are observed, while under pulsed irradiation a higher density of TEM-visible loops is predicted instead. In previous simulation work [17] it was shown that the reduced mobility of SIA clusters with Cr is the most important parameter driving the microstructure evolution of F/M steels under neutron irradiation, strongly influencing the recombination ratio between SIA and Va defect objects, which was observed to increase already with the addition of low Cr concentrations. Moreover, the fact that the same trends of Figure 3 are also observed to be reproduced by the Va cluster populations strengthens the hypothesis that also in this case the different recombination ratio between the two irradiation regimes in the presence of Cr might play a key role.

Figure 4 shows the difference, in percentage, in the total number of recombination events that occur under continuous and pulsed irradiation, for both Fe-C and Fe-9%Cr-C, as a function of the accumulated dose. We can see that our OKMC model predicts more recombinations under continuous irradiation in Fe-C (positive values), while the trend is reversed in Fe-9%Cr-C where the number of recombinations that occur under pulsed irradiation is larger (negative values).

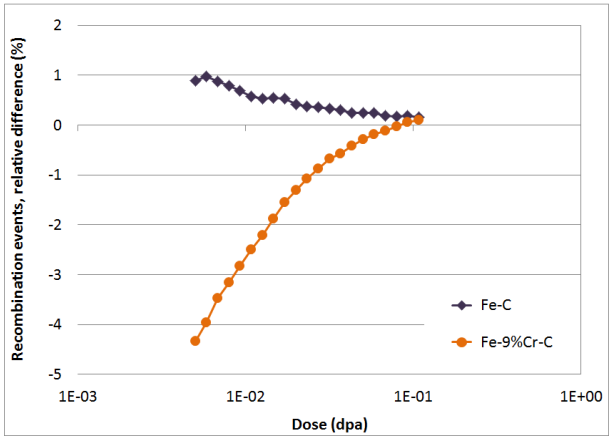

Figure 4: Comparison between Fe-C and Fe-9%Cr-C model alloys: difference between the total number of recombination events that occur under continuous and under pulsed irradiation, as a function of the accumulated dose (in %). Positive values indicate more recombinations under continuous irradiation than pulsed, negative values the opposite.

Figure 5 shows the difference, in percentage, between the total number of recombinations that occur in Fe-9%Cr-C and in Fe-C, for continuous and pulsed irradiation, as a function of the accumulated damage. Clearly, a higher amount of recombinations occur in Fe-9%Cr-C with respect to Fe-C when the pulsed irradiation regime is applied, while under continuous irradiation this becomes true only for high enough dose. This result suggests that the difference in the recombination ratio, which is strongly correlated to the different response to the two irradiation regimes of the investigated model alloys, depends on the time required for the different events to occur. More specifically, under pulsed irradiation the annealing time between successive pulse packets allows both SIA and Va defect objects to migrate further, thereby enhancing the probability for recombinations. This phenomenon is more evident in the case of Fe-9%Cr-C, where SIA clusters are significantly slowed down by the presence of Cr and are thus able to migrate further only if the lapse of time before the injection of new cascade in the neighbourhood is long enough. In the Fe-C model, in contrast, small SIA defects diffuse fast enough not to see a difference in the defect cluster nanostructure evolutions when the two irradiation regimes are applied.
Finally, the fact that the differences in the recombination ratios are observed to fade away with increasing dose is a consequence of the formation of a greater population of larger (and therefore slower) defect clusters, whose diffusivity is less sensitive to the presence of Cr.

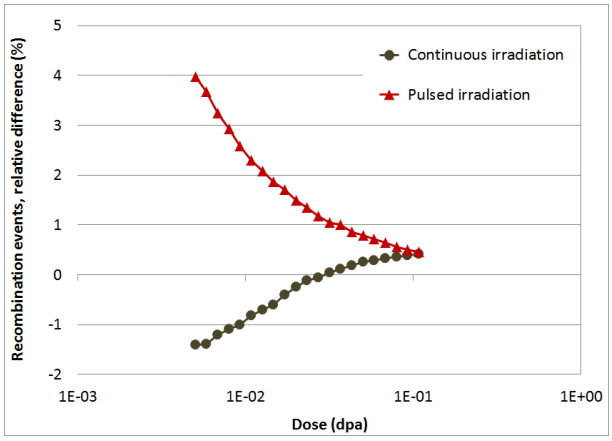

Figure 5: Comparison between pulsed and continuous irradiation: difference between the total number of recombination events that occur in Fe-9%Cr-C and in Fe-C (in %), as a function of the accumulated dose. Positive values indicate more recombination in Fe-9%Cr-C, while negative values indicate more recombinations in Fe-C.

Discussion and conclusions

The main cause of the different damage microstructures observed after the same accumulated dose under neutron and ion irradiation is to be attributed to the difference in dose-rate, which was seen to affect the initial distribution of defects and their subsequent evolution under irradiation. Higher fluxes induce the formation of a larger amount of (smaller) SIA defect clusters inside the grain, which can represent nucleation points for other migrating clusters or solute atoms dragged by point-defects [35].

However, the applied dose-rate is not the only difference between ion and neutron irradiation. The proximity of a surface, the injection of interstitials, or the presence of a damage gradient along the irradiation depth, are expected to have an effect too.

Here we have taken into account the effect of pulsed irradiation, consequent to the use of a scanning ion beam. We have shown that this may or may not lead to a different material microstructure response, depending on the diffusion properties of radiation defects in the specific irradiated alloy. Notably, the increased recombination ratio between Va and SIA defects, purportedly due to the presence of Cr, leads to a higher sensitivity to changes in the irradiation regime: in ferritic/martensitic steels Cr enhances the defect cluster recombination ratio much more than in Fe. This mechanism becomes even more evident under pulsed ion irradiation, where the annealing time between successive pulse packets somehow "averages" the higher dose-rate associated to the beam pulses and leads to lower defect cluster densities, the critical parameter determining whether or not the annealing between pulses has an effect being, as we have seen, the relative difference in diffusivity between SIA- and Va-type defects.

An accompanying effect not addressed here, though, is the likely temporary increase of local temperature when the ion beam pulse is focused on a small spot, which may have further influence on the evolution and either enhance or offset the effect of pulsed irradiation versus continuous.

Acknowledgements

The research leading to these results is partly funded by the European Atomic Energy Community's (Euratom) Seventh Framework Programme FP7/2007-2013 under grant agreement No. 604862 (MatISSE project) and contributes to the Joint Programme on Nuclear Materials (JPNM) of the European Energy Research Alliance (EERA).

References

[1] H. Tanigawa, K. Shiba, A. Moeslang, R.E. Stoller, R. Lindau, M.A. Sokolov, G.R. Odette, R.J. Kurtz, S. Jitsukawa (2011), J. Nucl. Mater., 417, pp. 9-15.

[2] T.R. Allen, J.T. Busby, R.L. Klueh, S.A. Maloy, M.B. Toloczko (2008), JOM, 60, pp. 15-23.

[3] Y.-I Kim, Yong Bum Lee, Chan Bock Lee, Jinwook Chang, Chiwoong Choi (2013), Sci. Technol. Nucl. Install., 2013, pp. 290-362.

[4] E.A. Little, D.A. Stow (1979), J. Nucl. Mater., 87, pp. 25-39.

[5] S. Porollo, A. Dvoriashin, A. Vorobyev, Y. Konobeev (1998), J. Nucl. Mater., 256, pp. 247-253.

[6] F.A. Garner, M.B. Toloczko, B.H. Sencer (2000), J. Nucl. Mater., 276, pp. 123-142.

[7] Y. Konobeev, A. Dvoriashin, S. Porollo, F. Garner (2006), J. Nucl. Mater., 355, pp. 124-130.

[8] M. Lambrecht, L. Malerba (2011), Acta Mater., 59, pp. 6547-6555.

[9] A. Fry, S. Osgerby, M. Wright (2002), "Oxidation of alloys in steam environment – a review", National Physics Laboratory Report NPL MATC(A)90.

[10] R.L. Klueh , D.R. Harries (2001), "High Chromium Ferritic and Martensitic Steels for Nuclear Applications", ASTM, West Conshohocken, PA.

[11] T. Okita, T. Sato, N. Sekimura, F.A. Garner, L.R. Greenwood (2002), J. Nucl. Mater., 322, pp. 307–311.

[12] F.A. Garner, D.S. Gelles, L.R. Greenwood, T. Okita, N. Sekimura, W.G. Wolfer (2004), J. Nucl. Mater., 1008, pp. 329–333.

[13] T. Okita, T. Sato, N. Sekimura, T. Iwai, F.A. Garner (2007), J. Nucl. Mater., 930, pp. 367–370.

[14] A.D. Amayev, A.M. Kryukov, V.I. Levit, M.A. Sokolov (1993), "Radiation stability of VVER-440 vessel materials", in: L.E. Steele (Ed.), Radiation Embrittlement of Nuclear Reactor Pressure Vessel Steels: An International Review, ASTM STP 1170, ASTM, Philadelphia, pp. 9–29.

[15] C.D. Hardie, C.A. Williams, S. Xu, S.G. Roberts (2013), J. Nucl. Mater., 439, pp. 33-40.

[16] V. Jansson, M. Chiapetto, L. Malerba (2013), J. Nucl. Mater., 442, pp. 341-349.

[17] M. Chiapetto , L. Malerba , C.S. Becquart (2015) , J. Nucl. Mater., 465, pp. 326–336.

[18] M. Chiapetto, C.S. Becquart, L. Malerba (2016), "Simulation of nanostructural evolution under irradiation in Fe-9%Cr-C alloys: an object kinetic Monte Carlo study of the effect of temperature and dose-rate", Nucl. Mater. Energy, In press.

[19] C. Domain , C. Becquart , L. Malerba (2004), J. Nucl. Mater., 335, pp. 121–145.

[20] V. Jansson , L. Malerba (2013) , J. Nucl. Mater., 443, pp. 274–285.

[21] A.B. Bortz , M.H. Kalos , J.L. Lebowitz (1975), J. Comput. Phys., 17, pp. 10–18 .

[22] W. Young , E. Elcock (1966), Proc. Phys. Soc., 89, pp. 735-746 .

[23] C. Domain, C. Becquart, L. Malerba (2004), in: N. Ghoniem (Ed.), Proceedings of Second International Conference on Multiscale Materials Modeling: October 11-15, 2004, Mechanical and Aerospace Engineering Department, University of Calif., Los Angeles, California.

[24] F. Nichols (1978), J. Nucl. Mater., 75, pp. 32-41.

[25] R. Stoller (1996), J. Nucl. Mater., 233, pp. 999–1003 .

[26] R. Stoller, G. Odette, B. Wirth (1997), J. Nucl. Mater., 251, pp. 49–60 .

[27] R. Stoller, A. Calder (2000), J. Nucl. Mater., 283, pp. 746–752 .

[28] M. Norgett, et al. (1975), Nucl. Eng. Des., 33, pp. 50-54.

[29] C. Domain, C. Becquart, L. Malerba (2004), J. Nucl. Mater., 335, pp. 121–145.

[30] M. Matijasevic, Ph.D.thesis, University of Ghent, 2007.

[31] L. Malerba (2011), Experimental reference cases for model validation in Fe and FeC alloys, Technical Report, Public Deliverable Nr. D1-3.10, FP7/Perform60 Collaborative Project, Grant Agreement Nr. FP7-232612.

[32] C. Heintze (2016). Private communication.

[33] L. Malerba, C.S. Becquart, C. Domain (2007), J. Nucl. Mater., 360, pp. 159–169 .

[34] M. Hernández-Mayoral , C. Heintze , E. Oñorbe (2016), J. Nucl. Mater., 474, pp. 88–98 .

[35] L. Messina, M. Nastar, T. Garnier, C. Domain, P. Olsson (2014), Phys. Rev. B, 90, 104203.